Mineralogical Magazine, February 2015, Vol. 79(1), pp. 157–170

Thermal behaviour of alum-(K) $KAl(SO_4)_2{\cdot}12H_2O$ from *in situ* laboratory high-temperature powder X-ray diffraction data: thermal expansion and modelling of the sulfate orientational disorder

PAOLO BALLIRANO*

Dipartimento di Scienze della Terra, Sapienza Università degli Studi di Roma, Piazzale Aldo Moro 5, I-00185, Rome, Italy

[*Received 25 March 2014; Accepted 15 July 2014; Associate Editor: E. Grew*]

ABSTRACT

The present work analyses the thermal behaviour of alum-(K), $KAl(SO_4)_2{\cdot}12H_2O$, by *in situ* laboratory high-temperature powder X-ray diffraction data from 303 K to melting, which starts at 355 K and is completed, due to kinetics, at 359 K. The calculated a_0 linear thermal expansion coefficient is of $14.68(11) \times 10^{-6}$ K^{-1} within the investigated thermal range. The *k* disorder parameter, describing the extension of the orientational disorder of the sulfate group, has been found to decrease from ~0.70 to ~0.65 just before melting. It has been demonstrated that the occurrence of the disorder implies the coexistence of K^+ ions in both six- and seven-fold coordination. This is necessary for assigning a reasonable bond-valence sum of 0.81 valence units (vu) to the 'average' K^+ ion a instead of 0.66 vu, which is obtained in the case of six-fold coordination alone. We can describe the temperature dependence of *k* from 93−355 K by means of the empirical equation $k = 0.798(12) + 2.5(11) \times 10^{-4}\ T - 1.9(2) \times 10^{-6}\ T^2$, which includes reference low-temperature data. Bond-valence analysis has shown that, on cooling, an increase of the *k* disorder parameter and shortening of the K−O2 bond distance act together to maintain constancy in the bond-valence sum at the K site, stabilizing the structure. Therefore, the need for keeping the 'average' K^+ ion at a reasonable bond-valence sum appears to be the driving force for the ordering process involving the sulfate group.

KEYWORDS: alum-(K), powder X-ray diffraction, Rietveld method, thermal behaviour, sulfate disorder.

Introduction

ALUM-(K), potassium aluminium sulfate dodecahydrate, $KAl(SO_4)_2{\cdot}12H_2O$, is a ubiquitously occurring sulfate, which has been mined actively for centuries for use in several industrial processes (water purification, dyeing, leather tanning etc.). It occurs as an alteration product of potassium-bearing rocks, pyritiferous shales and ignimbrites or from the oxidation of sulfureous gases in geothermal fields (Martin *et al*., 1999; Jambor *et al*., 2000). It is commonly associated with other metal-sulfate salts such as alunogen, halotrichite and melanterite. Alum-(K) is a member of the alum group, which comprises alum-(Na) $NaAl(SO_4)_2{\cdot}12H_2O$, lanmuchangite $Tl^+Al(SO_4)_2{\cdot}12H_2O$ and tschermigite $(NH_4)Al(SO_4)_2{\cdot}12H_2O$, plus the related phase lonecreekite $(NH_4)Fe^{3+}(SO_4)_2{\cdot}12H_2O$. At least a partial solid solution between tschermigite and lonecreekite has been reported (Martini, 1984). A large number of synthetic analogues, with general formula $M^IM^{III}(SO_4)_2{\cdot}12H_2O$, where M^I represents a monovalent metal (Cs, K, Na, Rb, Tl), a group such as NH_4, NH_3CH_3, or NH_3OH, M^{III} is a

* E-mail: paolo.ballirano@uniroma1.it
DOI: 10.1180/minmag.2015.079.1.13

trivalent metal (Al, Cr, Ga, In, Ru etc.) and S may be substituted by Se, have been prepared and structurally characterized (Abdeen *et al*., 1981*a*,*b*; Best and Forsyth, 1990*a*,*b*, 1991; Figgis *et al*., 2000; Nyburg *et al*., 2000 among others).

The aim of this present work, which is framed within a well-established research project on the crystal chemistry and thermal stability of hydrated sulfates (Ballirano, 2006; Carbone *et al*., 2008; Ballirano and Melis, 2009), is to investigate, using *in situ* high-temperature laboratory parallel beam powder X-ray diffraction (HT-PXRD), the thermal expansion and the structural modifications of alum-(K) that occur from room temperature (RT) to melting, with particular attention to the analysis of the sulfate group orientational disorder. A rationalization of the ordering process, taking into account the available low-temperature data, will be proposed and validated by the bond-valence method (Brown, 2002). Diffraction patterns were measured in transmission mode on a sample prepared as a capillary mount. The experimental set-up used in this investigation was chosen for its capability to produce high-quality diffraction data, at the same level as synchrotron radiation beamlines (Ballirano, 2011). Diffraction patterns are virtually texture-free and measured under conditions of excellent thermal stability and limited thermal gradient onto the capillary. In particular, the latter condition is crucial for investigating structural evolutions occurring within small, near RT, thermal ranges, requirements that are met with extreme difficulty by single-crystal X-ray structure refinement (SCSR).

Crystal structure of alum-(K)

The crystal structure of alum-(K) was first described by Cork (1927) and revised subsequently by Beevers and Lipson (1934). It crystallizes in the cubic space group $Pa\bar{3}$, with an a parameter of ~12.15 Å.

Alums are commonly subdivided into α-, β- or γ-type depending on the orientation of the sulfate group with respect to the unit cell, which essentially is guided by the size of M^{I}. In particular, alum-(K) is classified as an α-alum and it contains $\{Al(H_2O)_6\}$, $\{K(H_2O)_6\}$ and SO_4-groups connected by hydrogen bonding (Hawthorne *et al*., 2000). Its structure has received significant attention in the past owing to the peculiar orientational disorder of the sulfate group (Larson and Cromer, 1967). This disorder consists of the occurrence of two very close configurations, differing by ~0.5 Å, related by a reflection plane normal to the threefold axis and passing through the sulfur atom. At RT the two orientations have a well-defined population, which is in a 70:30 proportion (probability ratio $p_1/p_2 = 2.33$). The more probable one (hereinafter labelled as SO) consists of oxygen atoms O3 and O4 × 3, whereas the other one (hereinafter labelled as SOA) consists of oxygen atoms O3A and O4A × 3. This feature has been demonstrated to exist in a large number of $M^{I}M^{III}(SO_4)_2{\cdot}12H_2O$ alums, albeit with different probability ratios, of which magnitudes seem to depend, to some extent, on the ionic radius of the monovalent M^{I} cation (Nyburg *et al*., 2000). However, it is unclear what the crystal-chemical reason is for the occurrence of such disorder.

A few studies aimed at investigating the thermal behaviour of alum-(K), performed mainly using Raman spectroscopy, have revealed the increased ordering at SO as temperature is reduced from RT (Eysel and Schumacher, 1977; Sood *et al*., 1981; Brooker and Eysel, 1990). Such ordering has been identified by the analysis of the integrated intensities of the $\nu_1(SO_4)$ doublet occurring because of the presence of the two types of sulfate groups. The intensity ratio of the two components of the split A_g internal mode of sulfate has been related directly to the probability ratio p_1/p_2 (Sood *et al*., 1981) in good agreement with the SCSR carried out at RT by Larson and Cromer (1967). In effect, SCSR reports the site occupancy factor (s.o.f.) of the O3=O4 oxygen sites, otherwise referred to as the k disorder parameter, that corresponds to the fraction of tetrahedra in SO orientation. Subsequently, this agreement has been confirmed from SCSR carried out at 173 and 296 K (Nyburg *et al*., 2000). Raman measurements, collected within the 93 K < T < 297 K thermal range, indicate a significant departure from an exponential Boltzmann (two-level) distribution, of the area ratio, for T < 200 K (Sood *et al*., 1981). With respect to thermal behaviour at temperatures exceeding RT, no structural information is available, except for the melting temperature, which is 359 K as determined from differential thermal analysis data by Naumann and Emons (1989).

Experimental

Alum-(K) was synthesized by dissolution of equimolar amounts of $Al_2(SO_4)_3{\cdot}18H_2O$

(alunogen: purum p.a. Fluka 06421) and K_2SO_4 (arcanite: purum p.a. Fluka 60533) in distilled water, allowing slow evaporation at RT of the solvent water. The resulting crystals were ground in an agate mortar and the powder was charged in a borosilicate-glass capillary of 0.7 mm diameter that was glued to a 1.2 mm diameter Al_2O_3 tube using an alumina ceramic.

Data were collected in transmission mode, using Cu*K*α radiation, with a Bruker AXS D8 Advance Diffractometer operating in θ/θ geometry. The instrument is fitted with a prototype of a capillary heating chamber (Ballirano and Melis, 2007) that was calibrated using MgO (periclase) as standard (Reeber *et al*., 1995). Diffraction data were collected in the 10−140º2θ angular range with a step-size of 0.022º2θ, and 2 s of counting time, corresponding to ~3.5 h per pattern (Fig. 1). Data were measured isothermally in the 303−383 K thermal range at temperature steps of 4 K. Thermal stability is ±1 K. Temperature was raised at a rate of 0.1 K/s, waiting 60 s after the target temperature was attained before starting the measurement. The irradiated length of the capillary is ~8 mm and, within the investigated temperature range, a thermal gradient of <0.1 K/mm may be estimated, arising from the fact that the goniometer head is placed outside the chamber. In fact, a thermal gradient of ~0.5 K/mm has been observed at the α-quartz → β-quartz transition from the persistence of the low-*T* phase in a mixture with the high-*T* phase above the transition temperature. No Bragg reflections were observed at *T* >355 K indicating the occurrence of melting, which is confirmed by a significant increase of the background.

Diffraction patterns were evaluated by the Rietveld method using *TOPAS V.4.2* (Bruker AXS, 2009). To model the microstructure effects, the Double-Voigt Approach was used (Balzar, 1999), where crystallite size and strain comprise Lorentzian and Gaussian component convolutions varying in 2θ as a function of 1/cosθ and tanθ, respectively. The background was fitted with a Chebyshev polynomial of the first kind. Absorption was refined following a standard formalism for a cylindrical sample (Sabine *et al.*, 1998). Starting structural data were taken from Nyburg *et al*. (2000). Due to the strong correlation existing between them, the absorption parameter was initially refined by keeping the displacement parameters fixed to reference data and, subsequently fixed to allow for refinement of the individual displacement parameters (Ballirano and Maras, 2006). Preferred orientation was modelled by means of spherical harmonics (Järvinen, 1993). Selection of the number of terms was performed following the procedure described by Ballirano (2003).

A first series of refinements was carried out optimizing the spherical harmonics terms that were found to be extremely small (as expected for a capillary mount) and constant throughout the analysed thermal range. The final structural data set was obtained by keeping the spherical harmonics terms fixed to the corresponding average values (four spherical harmonics terms up to the 8th order: k41 = −0.014(3); k61 = −0.026(5); k62 = −0.006(8); k81 = 0.036(6), values between round brackets refer to data dispersion). The hydrogen-atoms position and displacement parameters were kept fixed to the corresponding value of reference data throughout the refinements. Refined parameters included fractional coordinates, individual isotropic displacement parameters for all non-hydrogen atoms

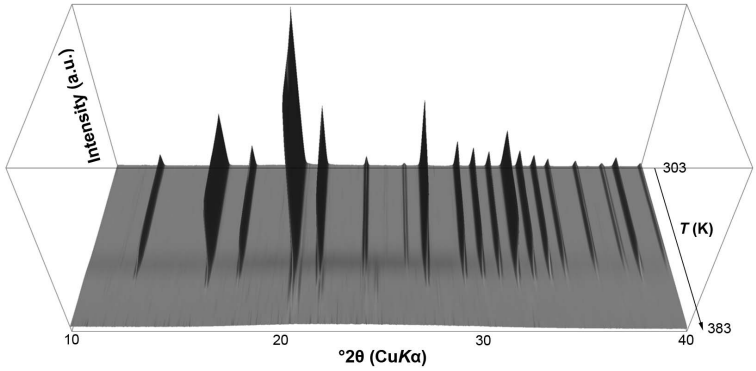

FIG. 1. Magnified 3D-view of the full PXRD data set from the heating experiment on alum-(K).

TABLE 1. Experimental details of the data collection.

Instrument	AXS Bruker D8 Advance Diffractometer
Optics	Multilayer graded (Göbel) mirrors
Slits	Soller ×2 (incident: 2.3º; diffracted: radial)
Detector	PSD VÅNTEC-1D
Radiation	Cu$K\alpha$
2θ range (º)	10−140
Step size (º2θ)	0.022
Counting time (s)	2
Thermal range (K)	303−355

and s.o.f. of the oxygen sites O3, O4, O3A and O4A. Besides, the constraints, O3=O3A and O4=O4A, were imposed on the displacement parameters in order to reduce correlations among s.o.f. and positional and displacement parameters due to the occurrence of two different SO_4-group orientations. Finally, no restraints on individual bond distances were imposed. A structure refined at a given temperature was used as input for the subsequent structure. Experimental details of data collection and conventional statistic indicators of the refinements are reported in Table 1 and 2, respectively. An example of Rietveld plots of the diffraction patterns collected at 311 and 351 K are shown in Fig. 2*a*,*b*.

Results and discussion

The relevant bond distances of alum-(K) at 303 K are listed in Table 3, a representative set of fractional coordinates, isotropic displacement parameters and *k* disorder parameter at 307 K is reported in Table 4. As can be seen, the geometry of the more probable (SO) tetrahedron is even more distorted than reported in reference data (Nyburg *et al*., 2000), whereas the geometry of the less probable configuration (SOA) is very similar. Nevertheless, the <S−O> bond distances for the two statistically disordered tetrahedra are of 1.468 Å and 1.450 Å for SO and SOA, respectively, in excellent agreement with 1.466 Å and 1.450 Å reported by Nyburg *et al*. (2000).

TABLE 2. List of conventional agreement indices of the various refinements. The significant reduction of the values of R_{wp}, R_p and Gof for the refinement of the data measured at 355 K is caused by the progressive reduction of the intensity of the peaks due to incipient melting. Statistical indicators are as defined by Young (1993).

T (K)	R_{wp}	R_p	Gof	DWd
303	5.68	4.38	1.410	1.174
307	5.64	4.36	1.403	1.179
311	5.57	4.30	1.383	1.229
315	5.57	4.30	1.381	1.213
319	5.77	4.46	1.43	1.190
323	5.72	4.38	1.416	1.157
327	5.70	4.43	1.413	1.190
331	5.68	4.37	1.408	1.163
335	5.71	4.40	1.416	1.203
339	5.69	4.37	1.412	1.181
343	5.76	4.43	1.429	1.179
347	5.73	4.45	1.420	1.199
351	5.42	4.19	1.313	1.339
355	4.62	3.60	1.110	1.735

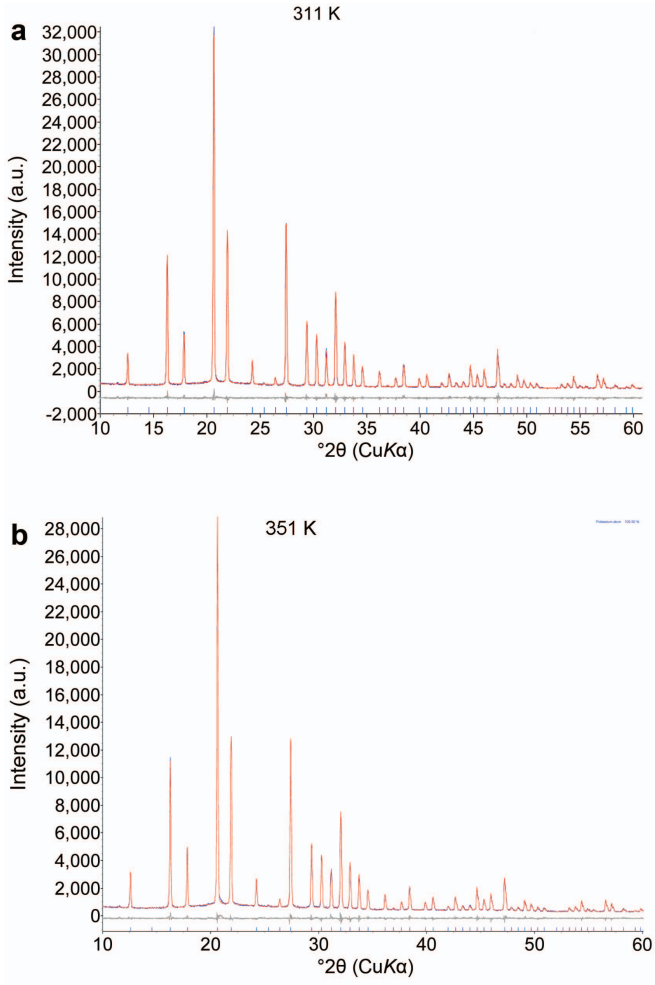

FIG. 2. Conventional Rietveld plots of the refinement of the diffraction data measured at (*a*) 311 K and (*b*) 355 K. Vertical bars refer to Bragg reflections of alum-(K).

Both values are fairly close to the average S–O bond distance of 1.48 Å found in sulfate groups occurring within inorganic compounds (Bergerhoff and Brandenburg, 1995) and the grand <S–O> distance of 1.473 Å observed in minerals (Hawthorne *et al*., 2000). Nyburg *et al*. (2000) attributed the shortening to the effect of libration. The marked distortion of both SO and, to a lesser extent, SOA tetrahedra, is possibly due to the effect of correlations among fractional coordinates, displacement parameters and s.o.f.

The Al–O bond distance is of 1.868(2) Å in good agreement with 1.875(1) Å from reference data.

The six K–O2 and the additional two K–O3A bond distances, the latter exclusively associated with the occurrence of the SOA orientation, were refined to 2.947(2) Å and 2.638(18) Å, respectively, compared to 2.954(1) Å and 2.636(5) Å of Nyburg *et al*. (2000). To date, no attention has been drawn to the anomalous situation resulting from calculations based on the parameters of Brese and O'Keeffe (1991), which give a bond-valence sum of only 0.66 vu for the six K–O2 bond distances, significantly less than the ideal value of 1. However, each KO_6 polyhedron is surrounded by eight SO_4 tetrahedra (Fig. 3*a*), two of which are at a suitable position for forming

TABLE 3. Relevant bond distances of alum-(K) at 303 K. The reference data of Nyburg *et al*. (2000) are reported for comparison.

	Present data	Nyburg *et al*. (2000)
S−O3	1.382(8)	1.447(4)
S−O4 × 3	1.497(5)	1.472(2)
<S−O>	1.468	1.466
S−O3A	1.417(18)	1.418(7)
S−O4A × 3	1.461(10)	1.460(4)
<S−OA>	1.450	1.450
Al−O1 × 6	1.8674(21)	1.8750(10)
K−O2 × 6	2.9473(24)	2.9540(10)
K−O3A × 1	2.638(18)	2.636(5)

extra K−O3A bonds whenever occupied by SOA (Fig. 3*b*). As each K−O3A bond provides a further 0.25 vu to K, a more conventional valence sum of 0.91 vu for a seven-fold coordination (one K−O3A, i.e. one SOA) or, alternatively, of 1.16 vu for an eight-fold coordination (two K−O3A, i.e. two SOA) may be obtained. Owing to the fact that the $Al(H_2O)_6$ polyhedron is moderately over-bonded (3.25 vu) it is expected that a seven-fold coordination, producing a slightly under-bonded KO_7 polyhedron, is favoured for providing an overall charge neutrality to the crystal. This reasoning is in contrast with the structural model proposed by Larson and Cromer (1967) indicating the occurrence of static disorder for potassium, which was allocated at two sites, K and K′. In fact, according to those authors, such disorder was required to justify the relatively high displacement parameters of K and to avoid the occurrence of a short K−O3A distance of ~2.68 Å that was present in the case of a single-site model. Accordingly, the occupancy of the K′ site was constrained to be equal to $k/2$ in order to correlate the occurrence of the K′ site with that of the SOA tetrahedron. Such a model results in two coordination polyhedra, the first one, KO_6, consisting of K−O2 × 6 at 2.983(9) Å, and a second, an almost regular $K'O_7$ consisting of K′−O2 × 3 at 2.92(2) Å, K′−O2 × 3 at 3.08(3) Å and K′−O3A at 2.98(12) Å. Unfortunately, both polyhedra produce bond-valence sums of 0.60 vu and 0.73 vu, respectively, significantly smaller than 1. On the contrary, present results indicate, from bond-valence analysis, that potassium in a distorted seven-fold coordination promotes the stabilization of the structure. An attempt to include the static disorder for K in the present refinement produced only minimal improvement of the agreement indices. The only structural difference with respect to the single-site model was, similarly to Larson and Cromer (1967), a symmetrization of the $K'O_7$ polyhedron causing a deleterious reduction, for the structure stability, of its bond-valence sum. Therefore, this model was discarded. Owing to the fact that each unit cell contains four K^+ ions and eight $SO_4^{=}$ groups, a seven-fold coordination may be extended to all

TABLE 4. Fractional coordinates, isotropic displacement parameters and *k* disorder parameter of alum-(K) at 307 K.

Site	*x*	*y*	*z*	U_{iso}	s.o.f.
S	0.30757(13)	0.30757(13)	0.30757(13)	0.0313(6)	1
Al	0	0	0	0.0200(9)	1
K	½	½	½	0.0510(10)	1
O1	0.15077(17)	0.02079(17)	−0.01958(18)	0.0251(9)	1
H1	0.198(0)	0.025(0)	0.038(0)	0.063(0)	1
H2	0.1752(0)	0.0350(0)	−0.0683(0)	0.063(0)	1
O2	0.04685(18)	0.1338(2)	0.30291(19)	0.0437(10)	1
H3	0.008(0)	0.184(0)	0.290(0)	0.063(0)	1
H4	0.104(0)	0.160(0)	0.299(0)	0.063(0)	1
O3	0.2426(4)	0.2426(4)	0.2426(4)	0.056(2)	0.660(4)
O4	0.2657(3)	0.4236(4)	0.3153(3)	0.0220(12)	0.660(4)
O3A	0.3764(8)	0.3764(8)	0.3764(8)	0.056(2)	0.340(4)
O4A	0.2627(6)	0.2063(8)	0.3656(6)	0.0220(12)	0.340(4)

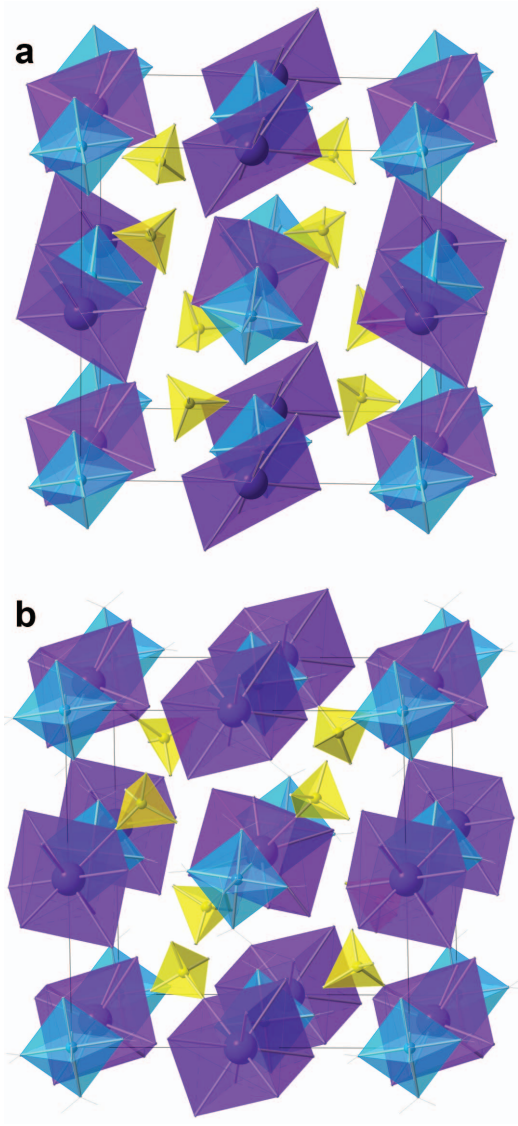

FIG. 3. Representation of the idealized structure of alum-(K) in the case of the exclusive occurrence of (*a*) SO tetrahedra and (*b*) SOA tetrahedra. Those configurations generate KO_6 or KO_8 polyhedra, respectively. Colour code: yellow = SO_4 tetrahedra; cyan = AlO_6 octahedra; indigo = KO_6 or KO_8 polyhedra.

K^+ ions only in the case of the occurrence of four SOA-type sulfates per unit cell, i.e. $k = 0.5$. Therefore, at RT the K^+ ions coexist in a statistically disordered distribution, in both six- and seven-fold coordination as a result of a k disorder parameter of ~0.7 (see below). An example of the seven-fold coordination of K^+ is reported in Fig. 4. Note that the K–O3A bond represents the only non-hydrogen bond polyhedral interconnection of the structure.

Isotropic displacement parameters are in good agreement with those of reference data, the exception being O3=O3A and, especially, O4=O4A, that are moderately underestimated.

Finally, the k disorder parameter has been refined to 0.666(4) at 303 K, a value slightly smaller than 0.697(5) reported at T = 296 K by Nyburg *et al*. (2000). A combined series of factors such as the underestimation of the O4=O4A displacement parameters, their reported moderate anisotropy (Nyburg *et al*., 2000), as well as the imposition of the two O3=O3A and O4=O4A constraints, plus the more accentuated distortion of the SO tetrahedron, could contribute to the minor reduction of the k parameter observed in the present refinement. At RT, the k order parameter of 0.70 corresponds to 2.40 SOA tetrahedra per unit cell available for bonding to four K^+ ions *via* O3A. This results in 60% of K^+ ions being in seven-fold and 40% in six-fold coordination. This population led to a bond-valence sum of 0.81 vu for the 'average' K^+ ion, a value that is acceptable and justified by the 'softness' of the K^+ cation, due to its ability to distort the electronic ground state in response to the surroundings (Bosi *et al*., 2009).

The dependence of the a cell parameter on temperature is reported in Fig. 5. The linear thermal expansion coefficient was calculated using the approach of Fei (1995) following the procedure described by Ballirano (2012), using an a parameter, a_{Tr}, at reference temperature T_r = 303 K of 12.15377(9) Å. The a_0 linear thermal expansion coefficient is $14.68(11) \times 10^{-6}$ K^{-1} for a determination coefficient R^2 = 0.9977. The a parameter at 303 K obtained in the present work is in good agreement with the value of 12.157(3) Å reported by Larson and Cromer (1967) but is significantly smaller than 12.1640(5) Å at 296 K as reported by Nyburg *et al*. (2000). The temperature dependence of bond distances, displacement parameters and a parameter is regular up to 351 K. Deviation from this trend is observed at 355 K, possibly due to precursor effects of melting. The <S–O> bond distances for the two statistically disordered tetrahedra are constant within the analysed thermal range, being 1.466(2) Å and 1.453(5) Å for the SO and the SOA configuration, respectively. Values between round brackets refer to data dispersion.

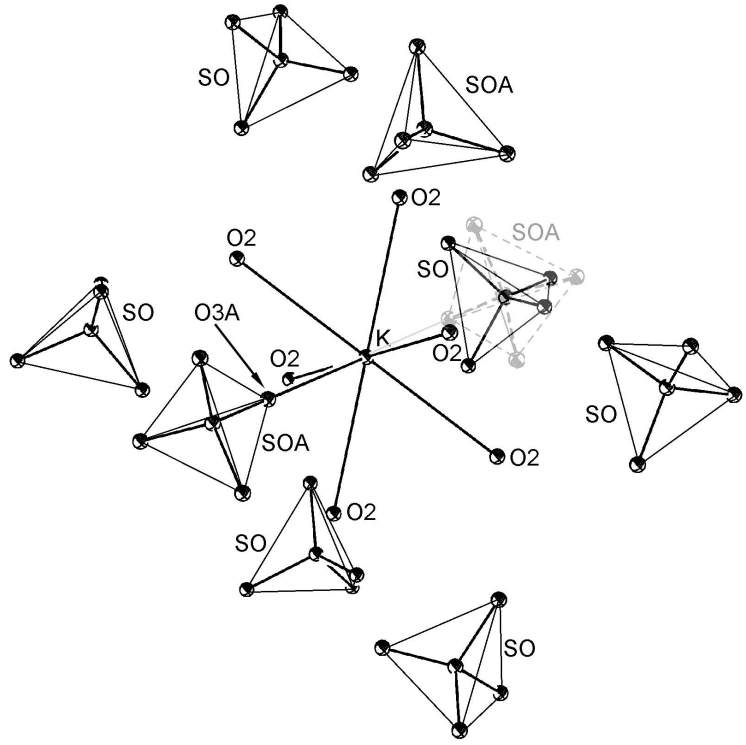

FIG. 4. *Ortep-3* (Farrugia, 1999) plot of the possible configuration of the sulfate groups for a *k* disorder parameter of 0.75, which is expected to occur, from reference Raman data (Sood *et al*., 1981), at a *T* of ~240 K. The non-occurring SOA tetrahedron, located at bonding distance from K *via* O3A, is plotted in grey.

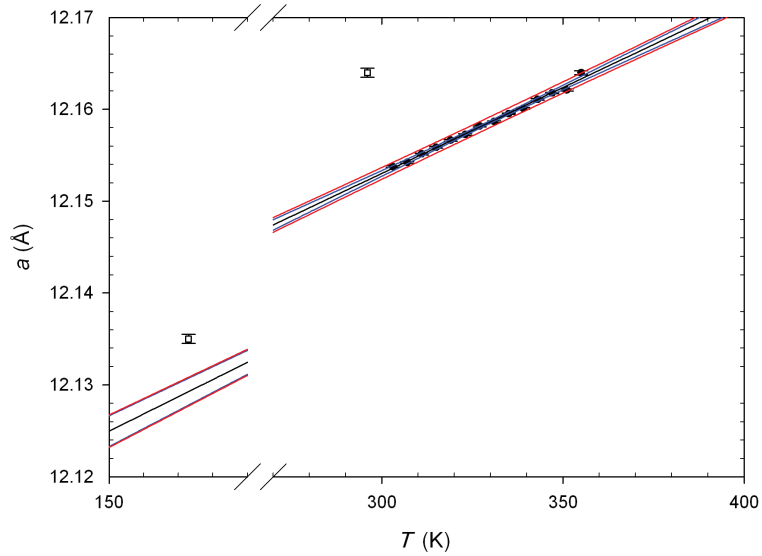

FIG. 5. Dependence of the *a* parameter of alum-(K) on temperature. Unfilled squares: data from Nyburg *et al*. (2000) from single-crystal structure refinements (SCSR). Error bars are smaller than symbols. Linear regression (black), 95% confidence (blue) and 95% prediction (red) plots are reported.

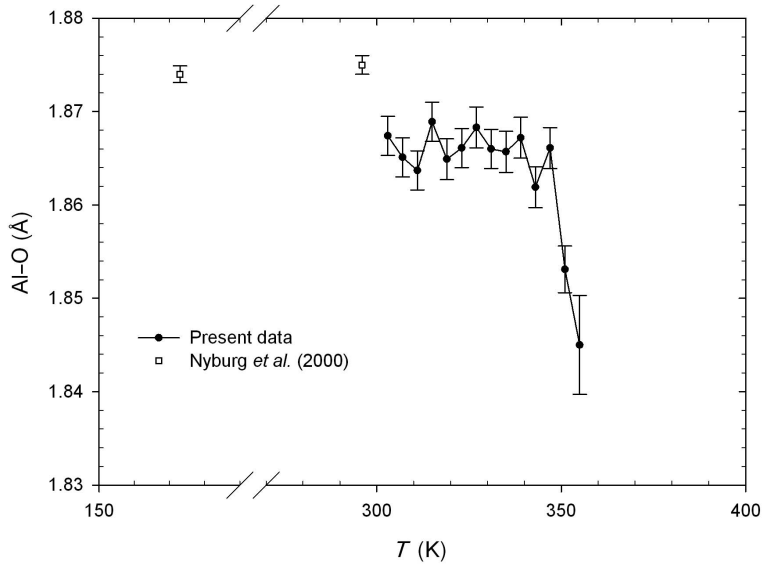

FIG. 6. Dependence of the Al–O bond distance on temperature.

Low-temperature data (Nyburg *et al*., 2000) point to more conventional values of 1.474 and 1.473 Å due to reduced librational motions of the tetrahedra. In contrast, the Al–O bond distance is constant up to 347 K (<Al–O> 1.866(1) Å) and subsequently decreases to 1.844(5) Å at 355 K (Fig. 6). The same independence from temperature has been observed in reference SCSR data which report bond distances of 1.8740(9) Å measured at 173 K and 1.875(1) Å at 296 K (Nyburg *et al*., 2000). The K^+ cation experiences a limited elongation of the six K–O2 bond distances from 2.947(2) Å to 2.962(2) Å as an effect of heating (Fig. 7). This trend extends towards low temperatures as indicated by the shortening to 2.9151(9) Å reported for the

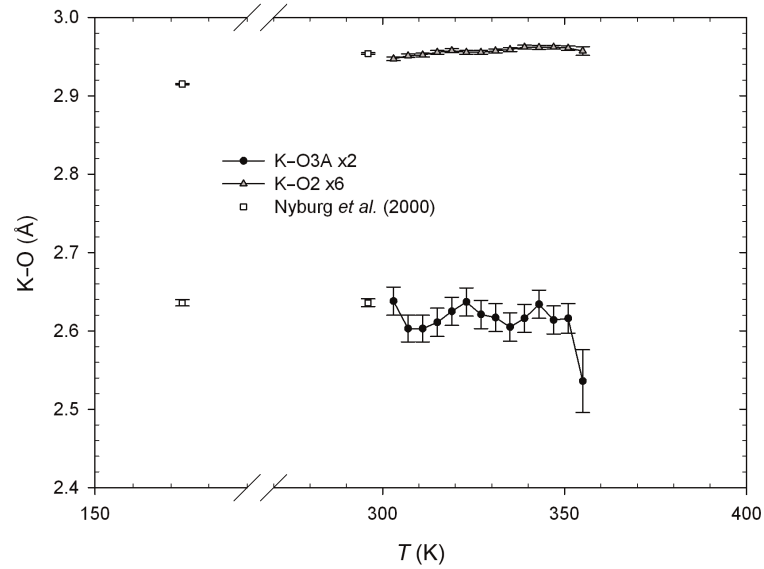

FIG. 7. Dependence of the K–O bond distances on temperature.

refinement at 173 K (Nyburg *et al*., 2000). In contrast, the K−O3A bond distance is substantially independent of *T*, even at low-temperatures.

As expected, the displacement parameters regularly increase as a function of *T* up to 347 K, and more rapidly at higher temperatures possibly as an effect of the incipient melting process (Fig. 8*a*,*b*).

The *k* disorder parameter has been found to vary linearly in the 303−355 K thermal range ($R^2 = 0.953$; $k = 0.883(16) - 7.2(5) \times 10^{-4}\ T$), the only exception being represented by the data point at 355 K. Note that the regression line runs perfectly parallel to the line passing through the SCSR data at 173 and 297 K (Nyburg *et al*., 2000) albeit systematically displaced by −0.026 (Fig. 9). Owing to the fact that s.o.f. derived from SCSR are expected to be more accurate than those from PXRD, the present data were rescaled, by adding 0.026, and merged with those of Sood

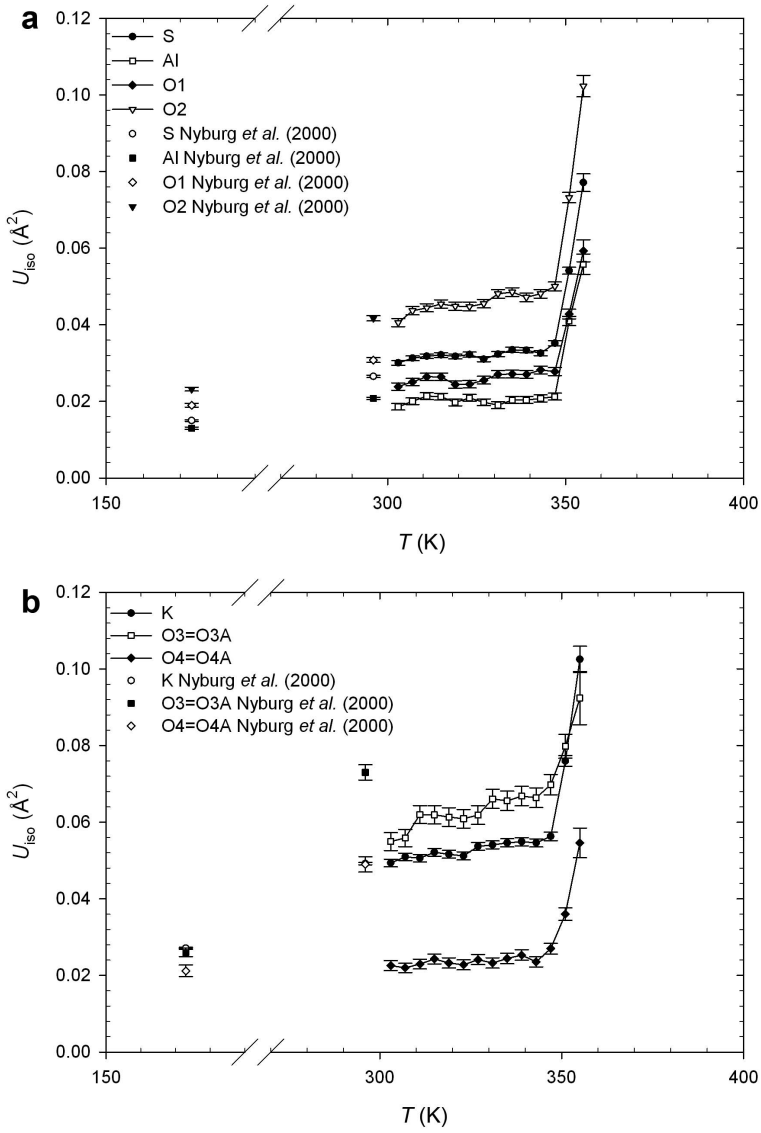

FIG. 8. Dependence of the U_{iso} isotropic displacement parameters of (*a*) S, Al, O1 and O2, (*b*) K, O3=O3A and O4=O4A on temperature.

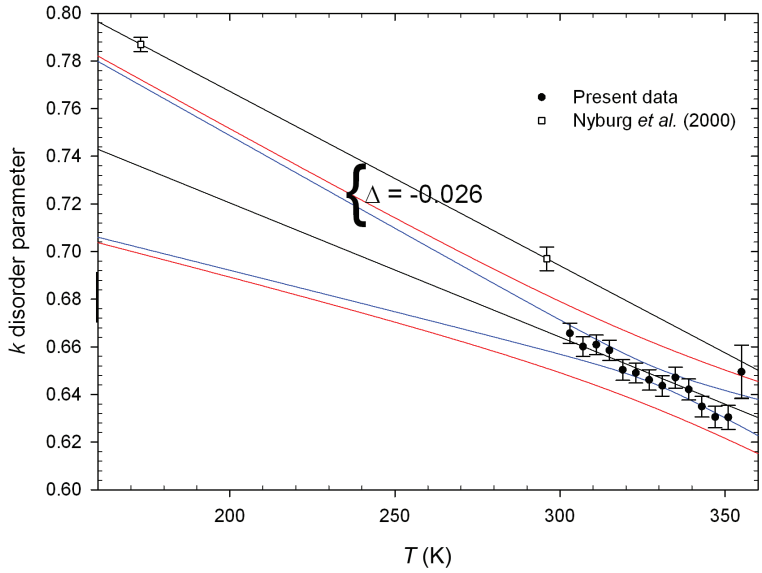

FIG. 9. Dependence of the *k* disorder parameter on temperature. Linear regression (black), 95% confidence (blue) and 95% prediction (red) plots are shown. The line passing through the two data points of Nyburg *et al*. (2000) is also shown.

et al. (1981) and Nyburg *et al*. (2000) for modelling the dependence of *k* on *T* in a wider thermal range (Fig. 10). The dependence is empirically described in the 93–355 K thermal range ($R^2 = 0.982$) by the equation $k = 0.798(12) + 2.5(11) \times 10^{-4}\, T - 1.9(2) \times 10^{-6}\, T^2$.

Furthermore, the analysis of the dependence on *T* of the O···O contacts describing hydrogen

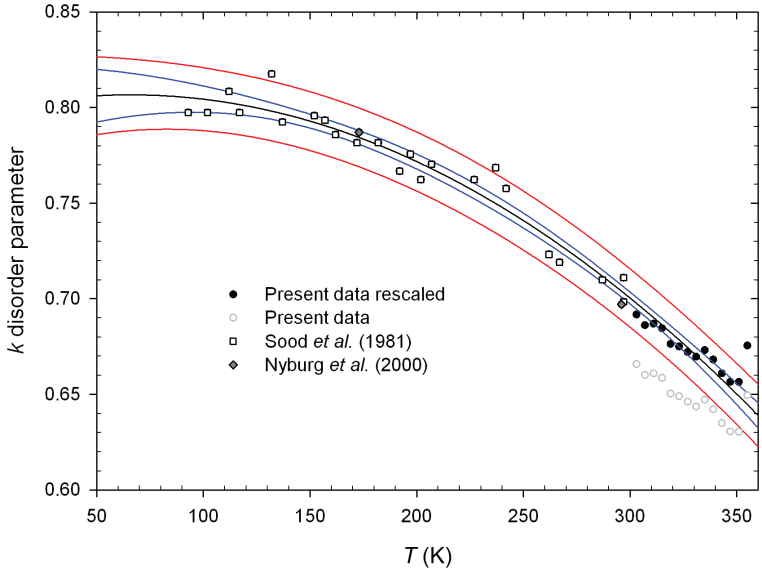

FIG. 10. Dependence of the *k* disorder parameter on temperature after the present data were rescaled and merged with those of Sood *et al*. (1981) and Nyburg *et al*. (2000). Regression equation (black), 95% confidence (blue) and 95% prediction (red) plots are shown.

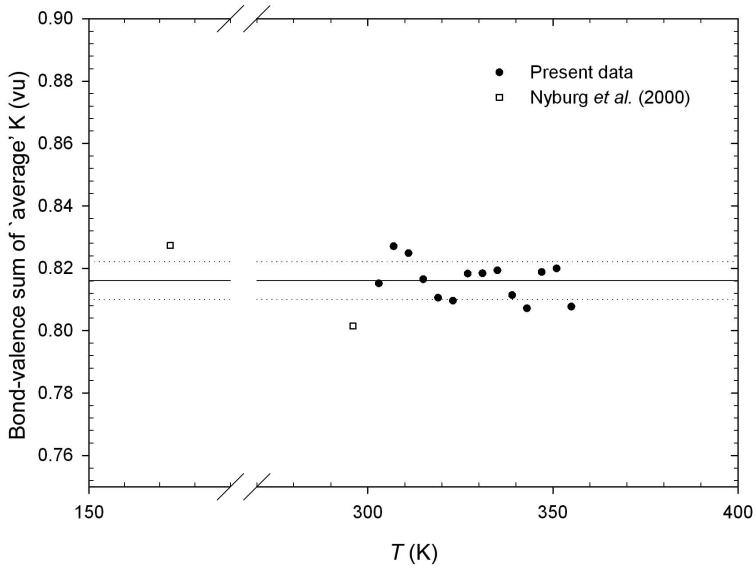

FIG. 11. Bond-valence sum at the 'average' K^+ ion calculated from the fraction of KO_6 and KO_7 polyhedra occurring at each *T*. The solid line represents the average value, whereas dotted lines represent the $\pm 1\sigma$ level.

bonds, was performed to check the correctness of the hypothesis raised by Nyburg *et al*. (2000) that hydrogen bonding contributes significantly to the total force field governing the particular orientations adopted by the sulfate groups. In detail, $\{Al(H_2O)_6\}$, $\{K(H_2O)_6\}$ and SO sulfate groups are connected by strong-to-medium hydrogen bonds (O1−H11···O4 and O1−H12···O2 = ~2.60 Å at RT and O2−H21···O3 and O2−H22···O4 at ~2.75 Å). In contrast, SOA is strongly linked to $\{K(H_2O)_6\}$ *via* K−O3A plus additional weak-to-very weak O2−H21···O4A (O2···O4A = ~2.9 Å at RT) and O2−H22···O4A (O2···O4A = ~3.1 Å at RT) hydrogen bonds. Besides, SOA is only weakly linked to $\{Al(H_2O)_6\}$ *via* O1−H11···O4A (O1···O4A = ~2.8 Å at RT). Data analysis revealed no significant variations within the analysed thermal range, the only relevant behaviour being the minor lengthening of both O2···O3 and O2···O4A (long) contacts, a trend that is consistent with the low-temperature data of Nyburg *et al*. (2000). As the connectivity of the SOA tetrahedron is assured mainly by K−O3A it could be speculated that the increasing weakening of the O2−H21···O3 hydrogen bond is responsible for a progressive destabilization of the structure as melting approaches.

An important result is represented by the observation that there is substantial independence from *T* of the bond-valence sum calculated for the 'average' K^+ ion, because a mean value of 0.816(7) vu (range 0.802−0.827) has been calculated in the 173−351 K thermal range (Fig. 11). Therefore, melting, which starts at 355 K, cannot be attributed to a destabilization of the KO_{6-7} polyhedron. On the contrary, increase of the *k* disorder parameter and shortening of the K−O2 bond distance together act to maintain constancy it the bond-valence sum at the 'average' K^+ ion, stabilizing the structure. This appears to be the driving force for the ordering process of the sulfate groups, occurring as temperature is reduced.

Acknowledgements

The author is grateful to Ed Grew, Peter Leverett and two anonymous reviewers for suggestions that significantly improved the quality of the paper. This work was funded by Sapienza Università di Roma.

References

Abdeen, A.M., Will, G. and Weiss, A. (1981*a*) Neutron diffraction study of alums. I. The crystal structure of hydroxilammonium aluminium alum. *Zeitschrift für Krystallographie*, **154**, 45−57.

Abdeen, A.M., Will, G., Schäfer, W., Kirfel, A.,

Bargouth, M.O., Recker, K. and Weiss, A. (1981*b*) Neutron diffraction study of alums. II The crystal structure of methylammonium aluminium alum. III The crystal structure of ammonium aluminium alum. *Zeitschrift für Krystallographie*, **157**, 147–166.

Ballirano, P. (2003) Effects of the choice of different ionization level for scattering curves and correction for small preferred orientation in Rietveld refinement: the $MgAl_2O_4$ test case. *Journal of Applied Crystallography*, **36**, 1056–1061.

Ballirano, P. (2006) Crystal chemistry of the halotrichite group $XAl_2(SO_4)_4{\cdot}22H_2O$: the X = Fe-Mg-Mn-Zn compositional tetrahedron. *European Journal of Mineralogy*, **18**, 463–469.

Ballirano, P. (2011) Thermal behaviour of natrite Na_2CO_3 in the 303–1013 K thermal range. *Phase Transitions*, **84**, 357–379.

Ballirano, P. (2012) The thermal behaviour of liottite. *Physics and Chemistry of Minerals*, **39**, 115–121.

Ballirano, P. and Maras, A. (2006) Mineralogical characterization of the blue pigment of Michelangelo's fresco "The Last Judgement". *American Mineralogist*, **91**, 997–1005.

Ballirano, P. and Melis, E. (2007) Thermal behaviour of β-anhydrite $CaSO_4$ to 1,263 K. *Physics and Chemistry of Minerals*, **34**, 699–704.

Ballirano, P. and Melis, E. (2009) Thermal behaviour and kinetics of dehydration in air of bassanite, calcium sulphate hemihydrate ($CaSO_4{\cdot}0.5H_2O$), from X-ray powder diffraction. *European Journal of Mineralogy*, **21**, 985–993.

Balzar, D. (1999) Voigt-function model in diffraction line-broadening analysis. Pp. 94–126 in: *Defect and Microstructure Analysis from Diffraction* (R.L. Snyder, H.J. Bunge and J. Fiala, editors). International Union of Crystallography Monograph on Crystallography **No. 10**, Oxford University Press, New York.

Beevers, C.A. and Lipson, H. (1934) Crystal structure of the alums. *Nature*, **134**, 327–327.

Bergerhoff, G. and Brandenburg, K. (1995) Interatomic distances: inorganic compounds. Pp. 683–684 in: *International Tables for Crystallography*, **Volume C** (A.J.C Wilson, editor). Kluwer Academic Publishers, London.

Best, S.P. and Forsyth, J.B. (1990*a*) Stereochemistry of tervalent aqua ions: low-temperature neutron diffraction structures of $CsFe(SO_4)_2{\cdot}12H_2O$ and $CsFe(SeO_4)_2{\cdot}12H_2O$. *Journal of the Chemical Society, Dalton Transactions*, **1990**, 395–400.

Best, S.P. and Forsyth, J.B. (1990*b*) Low-temperature neutron-diffraction structure of $[Ru(OH_2)_6]^{3+}$ in the caesium sulphate alum lattice $CsRu[SO_4]_2{\cdot}12H_2O$. *Journal of the Chemical Society, Dalton Transactions*, **1990**, 3507–3511.

Best, S.P. and Forsyth, J.B. (1991) Relationship between the electronic and molecular structure of tervalent aqua ions: low-temperature neutron diffraction structure of $CsCr(SO_4)_2{\cdot}12H_2O$. *Journal of the Chemical Society, Dalton Transactions*, **1991**, 1721–1725.

Bosi, F., Belardi, G. and Ballirano, P. (2009) Structural features in Tutton's salts $K_2[M^{2+}(H_2O)_6](SO_4)_2$, with M^{2+} = Mg, Fe, Co, Ni, Cu, and Zn. *American Mineralogist*, **94**, 74–82.

Breese, N.E. and O'Keeffe, M. (1991) Bond-valence parameters for solids. *Acta Crystallographica*, **B47**, 192–197.

Brooker, M.H. and Eysel, H.H. (1990) Raman study of sulfate orientational dynamics in α-potassium alum and in the deuterated and oxygen-18 enriched forms. *Journal of Physical Chemistry*, **94**, 540–544.

Brown, I.D. (2002) *The Chemical Bond in Inorganic Chemistry: the Bond Valence Model*. International Union of Crystallography Monograph on Crystallography **No. 12**, Oxford University Press, New York, 278 pp.

Bruker AXS (2009) *Topas V.4.2: General profile and structure analysis software for powder diffraction data*. Bruker AXS, Karlsruhe, Germany.

Carbone, M., Ballirano, P. and Caminiti, R. (2008) Kinetics of gypsum dehydration at reduced pressure: an energy dispersive X-ray diffraction study. *European Journal of Mineralogy*, **20**, 621–627.

Cork, J.M. (1927) The crystal structure of some of the alums. *Philosophical Magazine*, **4**, 688–698.

Eysel, H.H. and Schumacher, G. (1977) Dynamic sulfate disorder in potassium alum. A single crystal Raman study. *Chemical Physics Letters*, **47**, 168–170.

Farrugia, L.J. (1999) *ORTEP-3 for Windows*, University of Glasgow, Scotland.

Fei, Y. (1995) Thermal expansion. Pp 29–44 in: *A Handbook of Physical Constants, Mineral Physics and Crystallography* (J.A. Ahrens, editor), AGU Reference Shelf 2, Washington DC.

Figgis, B.N., Reynolds, P.A. and Sobolev, A.N. (2000) The structure of α-alums $RbCr(SO_4)_2{\cdot}12H_2O$ and $CsCr(SeO_4)_2{\cdot}12H_2O$ at 293 and 12 K. *Acta Crystallographica*, **C56**, 731–734.

Hawthorne, F.C., Krivovichev, S.V. and Burns, P.C. (2000) The crystal chemistry of sulfate minerals. Pp. 1–112 in: *Sulfate minerals – Crystallography, Geochemistry, and Environmental Significance* (C.N. Alpers, J.L. Jambor, and D.K. Nordstrom, editors). Reviews in Mineralogy & Geochemistry, **Vol. 40**. Mineralogical Society of America and the Geochemical Society, Washington DC.

Jambor, J.L., Nordstrom, D.K. and Alpers, C.N. (2000) Metal-sulfate salts from sulphide mineral oxidation. Pp. 303–350 in: *Sulfate minerals – Crystallography, Geochemistry, and Environmental Significance* (C.N. Alpers, J.L. Jambor and D.K.

Nordstrom, editors). Reviews in Mineralogy & Geochemistry, **Vol. 40**. Mineralogical Society of America and the Geochemical Society, Washington DC.

Järvinen, M. (1993) Application of symmetrized harmonics expansion to correction of the preferred orientation effect. *Journal of Applied Crystallography*, **26**, 525–531.

Larson, A.C. and Cromer, D.T. (1967) Refinement of the alum structures. III. X-ray study of the α alums, K, Rb and $NH_4Al(SO_4)_2 \cdot 12H_2O$. *Acta Crystallographica*, **22**, 793–800.

Martin, R., Rodgers, K.A. and Browne, P.R.L. (1999) The nature and significance of sulphate-rich aluminous efflorescences from Te Kopia geothermal field, Taupo volcanic zone. *Mineralogical Magazine*, **63**, 413–419.

Martini, J.E.J. (1984) Lonecreekite, sabieite, and clairite, new secondary ammonium ferric-iron sulfates from Lone Creek Fall cave, near Sabie, Eastern Transvaal. *Annals of the Geological Survey (South Africa)*, **17**, 29–34.

Naumann, R. and Emons, H.-H. (1989) Results of thermal analysis for investigation of salt hydrates as latent heat-storage materials, *Journal of Thermal Analysis and Calorimetry*, **35**, 1009–1031.

Nyburg, S.C., Steed, J.W., Aleksovska, S. and Petrusevski, V.M. (2000) Structure of the alums. I. On the sulphate group disorder in the α-alums. *Acta Crystallographica*, **B56**, 204–209.

Reeber, R.R., Goessel, K. and Wang, K. (1995) Thermal expansion and molar volume of MgO, periclase, from 5 to 2900 K. *European Journal of Mineralogy*, **7**, 1039–1047.

Sabine, T.M., Hunter, B.A., Sabine, W.R. and Ball, C.J. (1998) Analytical expressions for the transmission factor and peak shift in absorbing cylindrical specimens. *Journal of Applied Crystallography*, **31**, 47–51.

Sood, A.K., Arora, A.K., Dattagupta, S. and Venkataraman, G. (1981) Raman study of orientational dynamics of sulphate ions in potash alum. *Journal of Physics C: Solid State Physics*, **14**, 5215–5224.

Young, R.A. (1993) Introduction to the Rietveld method. Pp. 1–38 in: *The Rietveld Method* (R.A. Young, editor). Oxford University Press, Oxford.